$^3\overrightarrow{\mathrm{He}}(\vec{e}, e')X$ AND THE NEUTRON ELECTROMAGNETIC FORM FACTORS

J.-O. Hansen

Physics Division, Argonne National Laboratory,
Argonne, Illinois 60439-4843, USA.

ABSTRACT

Recent data for the spin-dependent $A_{T'}$ and $A_{TL'}$ asymmetries in $^3\vec{\mathrm{He}}(\vec{e}, e')$ quasielastic scattering are reviewed. The neutron electric and magnetic form factors are extracted from the data using a PWIA model, and the model uncertainties are estimated. The extracted G_M^n is in agreement with the dipole prediction as well as with other recent experiments. No meaningful result for G_E^n is obtained due to large uncertainties and possible final-state interaction effects. At higher Q^2, the determination of G_E^n in $^3\vec{\mathrm{He}}(\vec{e}, e')$ does appear feasible based on the PWIA predictions.

1. Introduction

A complete understanding of the electromagnetic structure of the nucleon requires knowledge of both the electric form factors (G_E^n and G_E^p) and the magnetic form factors (G_M^n and G_M^p) of the neutron and the proton. Accurate data on these fundamental quantities, which are directly related to the charge and magnetization distributions inside the nucleon, provide constraints on nucleon models based on QCD, as well as a basis for calculations of electromagnetic nuclear structure. While the proton form factors are experimentally rather well established[1], the neutron form factors are still subject to large uncertainties, largely due to the fact that no suitable free neutron targets are available. In the past, most information about G_M^n and G_E^n has been obtained in elastic and quasielastic electron scattering from deuterium[2,5,27,3], resulting in about $\pm 15\%$ accuracy for G_M^n and more than $\pm 50\%$ uncertainty for G_E^n. Only the slope of $G_E^n(Q^2)$ near zero momentum transfer Q^2 has been determined with high precision in neutron beam experiments[4].

Several new directions have been investigated lately to improve the precision of neutron form factor measurements. A novel technique[6–8] which involves the simultaneous measurement of the unpolarized $^2\mathrm{H}(e, e'n)$ and $^2\mathrm{H}(e, e'p)$ cross sections has

provided very high-quality data for G_M^n in the range $0.1 < Q^2 < 0.6$ (GeV/c)^2. Another approach is the use of polarization degrees of freedom in quasielastic (QE) electron scattering from deuterium and polarized ^{3}He ($^3\vec{\text{He}}$), which exploits the fact that certain spin observables are significantly more sensitive to small quantities, such as G_E^n, because they contain interference terms between the small charge and the larger magnetic multipoles. One example of this is the measurement of the neutron recoil polarization in $^2\text{H}(\vec{e}, e'\vec{n})$, which is expected to allow a largely model-independent extraction of G_E^n[9,10]. The experimental feasibility of this method has recently been demonstrated[12,11]. Polarized ^{3}He is an interesting nucleus for form factor studies because it may act as an effective polarized neutron target. Spin observables in QE scattering of polarized electrons from $^3\vec{\text{He}}$ therefore exhibit larger sensitivity to neutron electromagnetic properties than unpolarized observables[20]. Both inclusive scattering, $^3\vec{\text{He}}(\vec{e}, e')$[13–16], and the electron-neutron coincidence reaction, $^3\vec{\text{He}}(\vec{e}, e'n)$[17,18], have been investigated with the goal of extracting G_E^n and G_M^n. While the inclusive reaction is easier to study experimentally, it requires a model-dependent evaluation of the proton contribution to the spin observables. This is avoided in the coincidence technique, but one faces possible systematic uncertainties from final-state interactions (FSI) of the ejected neutron. Further discussion of the coincidence method is given in Refs.[17,18,29].

In this talk, I briefly review the results of the most recent $^3\vec{\text{He}}(\vec{e}, e')$ experiments[15,16] and then discuss the feasibility of determining the neutron electromagnetic form factors from this reaction in the region $0.1 < Q^2 < 1$ (GeV/c)^2. The theoretical results presented here were obtained in the framework of a plane wave impulse approximation (PWIA) calculation[24].

2. Physics Motivation

The differential cross section, σ, for spin-dependent electron scattering from a nuclear target can be expressed in terms of an unpolarized piece, Σ, and a polarized piece, Δ, so that $\sigma = \Sigma + h\Delta$, where $h = \pm 1$ is the helicity of the incident electrons. An experimentally clean signature of the polarized piece, which contains the spin observables of interest, is the spin-dependent asymmetry, defined as

$$A \equiv \frac{\sigma_{h=+1} - \sigma_{h=-1}}{\sigma_{h=+1} + \sigma_{h=-1}} = \frac{\Delta}{\Sigma}. \tag{1}$$

For elastic scattering from a free polarized neutron target, the polarized cross section is[19]

$$\Delta = -\cos\theta^* \tilde{v}_{T'} \, (G_M^n)^2 - 2 \sin\theta^* \cos\phi^* \tilde{v}_{TL'} \, G_M^n G_E^n \,, \tag{2}$$

where θ^* and ϕ^* are the polar and azimuthal angles defining the direction of the target spin with respect to the momentum transfer $\vec{q}$, and the $\tilde{v}_K$ are kinematic factors.

For inclusive electron scattering from the spin-$\frac{1}{2}$ ^{3}He target, on the other hand, the cross section depends on quasielastic response functions R_K. The spin-dependent

asymmetry for this reaction can be written[19]

$$A = -\frac{\cos\theta^* v_{T'} R_{T'}(Q^2,\omega) + 2\sin\theta^*\cos\phi^* v_{TL'} R_{TL'}(Q^2,\omega)}{v_T R_T(Q^2,\omega) + v_L R_L(Q^2,\omega)}, \quad (3)$$

where R_L and R_T are the familiar longitudinal and transverse response functions, respectively, and two additional response functions, a transverse response, $R_{T'}$, and an interference between transverse and longitudinal multipoles, $R_{TL'}$, completely describe the spin-dependent contribution to the cross section. These functions depend on the electron energy loss ω and the four-momentum transfer, $Q^2 \equiv |\vec{q}|^2 - \omega^2$. By orienting the target spin at $\theta^* = 90°$ (0°) one can select the asymmetry piece $A_{TL'}$ ($A_{T'}$) proportional to $R_{TL'}$ ($R_{T'}$).

At the quasielastic peak, the *polarized* piece of the ^{3}He cross section is expected to be dominated by the neutron because the ^{3}He ground state wave function is predominantly a spatially symmetric S state in which the spins of the two protons are antialigned and the nuclear spin is carried mainly by the unpaired neutron in the nucleus. Hence, the $^3\vec{\text{He}}$ responses $R_{TL'}$ and $R_{T'}$ should be sensitive to $G_M^n G_E^n$ and ${G_M^n}^2$, respectively.

This is confirmed in part by theoretical studies of inclusive QE scattering from $^3\vec{\text{He}}$. Recent analyses[21,22], which employ the PWIA to describe the scattering mechanism and use a full spin-dependent spectral function to model the $^3\vec{\text{He}}$ ground state, predict that about 90% of $A_{T'}$ stems from the neutron. Thus it should be possible to extract ${G_M^n}^2$ from $A_{T'}$. On the other hand, the studies show a dominant ($\sim 75\%$) proton contribution to $A_{TL'}$ at low $Q^2 \lesssim 0.2$ (GeV/c)^2, which greatly reduces the sensitivity to G_E^n. This proton contribution arises chiefly from the presence of the 'small' S' ($\sim 1\%$) and D ($\sim 8\%$) state admixtures to the ^{3}He ground state wave function, in which the protons contributes to the nuclear spin. FSI and meson-exchange current (MEC) effects are neglected in these studies.

3. Recent Data

The most recent data on inclusive scattering form $^3\vec{\text{He}}$ were taken in 1993 at the MIT-Bates Linear Accelerator Center (Experiment 88-25). The experiment employed a 370

Measurement	E (MeV)	E' (MeV)	$\|\vec{q}\|$ (MeV/c)	Q^2 (GeV/c)^2	θ	θ^*	ϕ^*
$A_{T'}$	370	250	452	0.20	91.4°	8.9°	180°
$A_{TL'}$	370	285	383	0.14	70.1°	87.0°	0°

TABLE 1. Kinematics of the recent MIT-Bates $^3\vec{\text{He}}(\vec{e},e')$ measurement. E: beam energy; E': scattered electron energy; θ: scattering angle. The other quantities are defined in the text.

MeV longitudinally polarized, pulsed electron beam and a low-density ^{3}He gas target[23] which was polarized by the metastability-exchange optical pumping technique. Both $A_{TL'}$ and $A_{T'}$ were measured at quasielastic kinematics, as detailed in Table 1. A full description of the experiment and analysis is given in Refs.[15,16].

The measured asymmetries are shown in Figs. 1 and 2 as a function of electron energy loss ω. The curves in the figures are the results of various PWIA calculations and are discussed in the next section.

4. Form Factor Extraction

Due to the complicated nature of the reaction dynamics and the physical $^3\vec{\mathrm{He}}$ ground state, the extraction of the neutron form factors from the measured $^3\vec{\mathrm{He}}(\vec{e},e')$ asymmetry data is not trivial and requires use of a model. Using the formalism of Refs.[22,25], the MIT-Hannover group[24] recently generated an extensive set of predictions for the $^3\vec{\mathrm{He}}(\vec{e},e')$ response functions in PWIA for a variety of input parameters. These calculations are used in the following.

To extract a value for G_E^n, predictions were computed for $A_{TL'}(G_E^n)$ (averaged over the experimental ω acceptance). G_E^n was taken to be a single input parameter constant over the energy acceptance, which is sufficiently accurate as G_E^n is expected to vary only slowly with Q^2. The dipole parameterization[27] was used for the other nucleon form factors. To estimate theoretical uncertainties, the predictions were generated for three different combinations of input parameters:

1. Paris NN potential[30] and CC1$^{(0)}$ single-nucleon off-shell prescription[25].
2. Reid soft-core NN potential[31] and the off-shell prescription used in Ref.[21].
3. Bonn B NN potential[32] and CC1$^{(0)}$ off-shell prescription.

These combinations were found to yield an intermediate value of, and an upper and lower bound on the asymmetry, respectively. The effect of different parameterizations of the other nucleon form factors is negligible compared to the variations arising from NN potential and off-shell prescription.

The three functions $A_{TL'}(G_E^n)$ obtained in this analysis are plotted in Fig. 3. The solid curve corresponds to case 1, the dashed curve to case 2, and the dot-dashed curve to case 3. The data point shown represents the measured asymmetry with total experimental error (arbitrarily placed at the Galster[27] value for G_E^n). The open circle on the x-axis is the extracted G_E^n value (-0.0015) obtained with calculation 1. The inner error bars represent the estimated theoretical uncertainty from different NN potentials and off-shell prescriptions (± 0.015); the middle error bars the experimental error (± 0.032); and the outer error bars the total uncertainty with theoretical and experimental uncertainty added linearly (± 0.047). The three open diamonds on the x-axis are the G_E^n predictions of Gari-Krümpelmann[28], Höhler[26], and Galster[27] at $Q^2 = 0.14$ (GeV/c)^2 (from left to right).

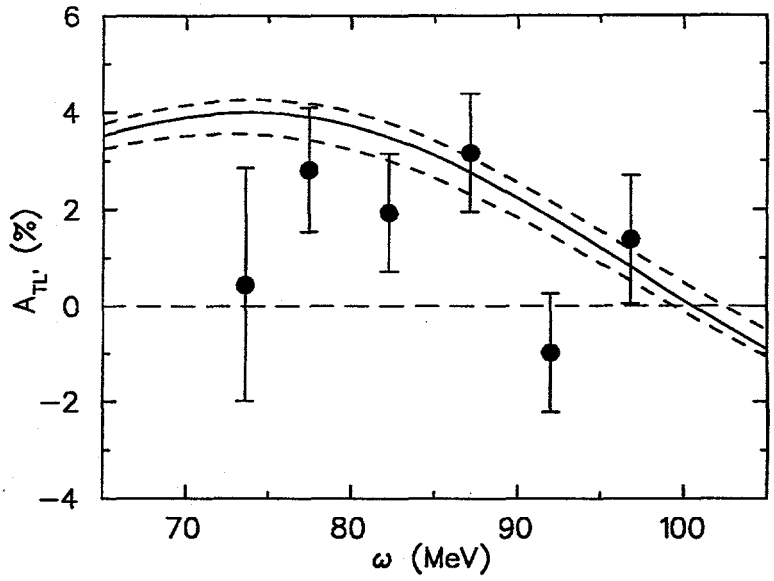

FIGURE 1. The transverse-longitudinal asymmetry, $A_{TL'}$, in $^3\vec{\mathrm{He}}(\vec{e},e')$ at $Q^2 = 0.14$ (GeV/c)^2 as a function of electron energy transfer. The data are from MIT-Bates experiment 88-25[16]. The errors are statistical only. The dashed curves represent the upper and lower limits of the present PWIA calculation (see text).

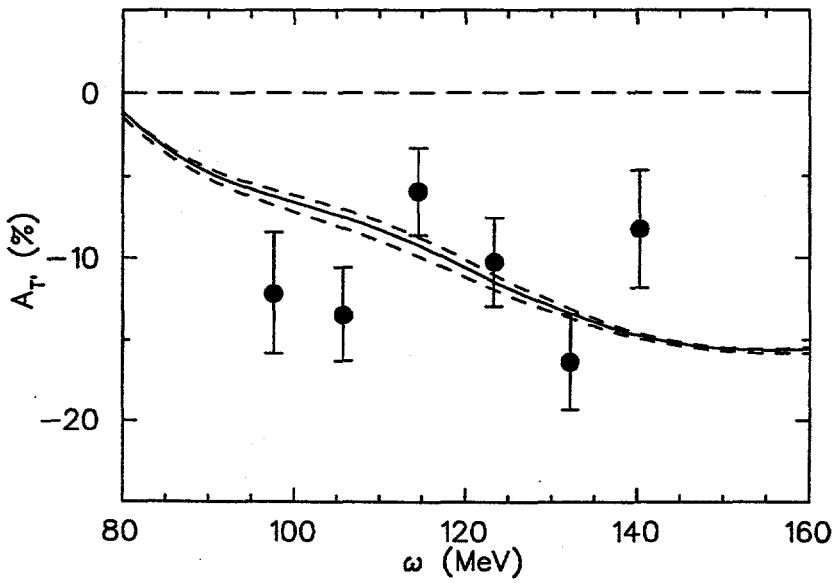

FIGURE 2. Same as Fig. 1 for the transverse asymmetry, $A_{T'}$, at $Q^2 = 0.20$ (GeV/c)^2.

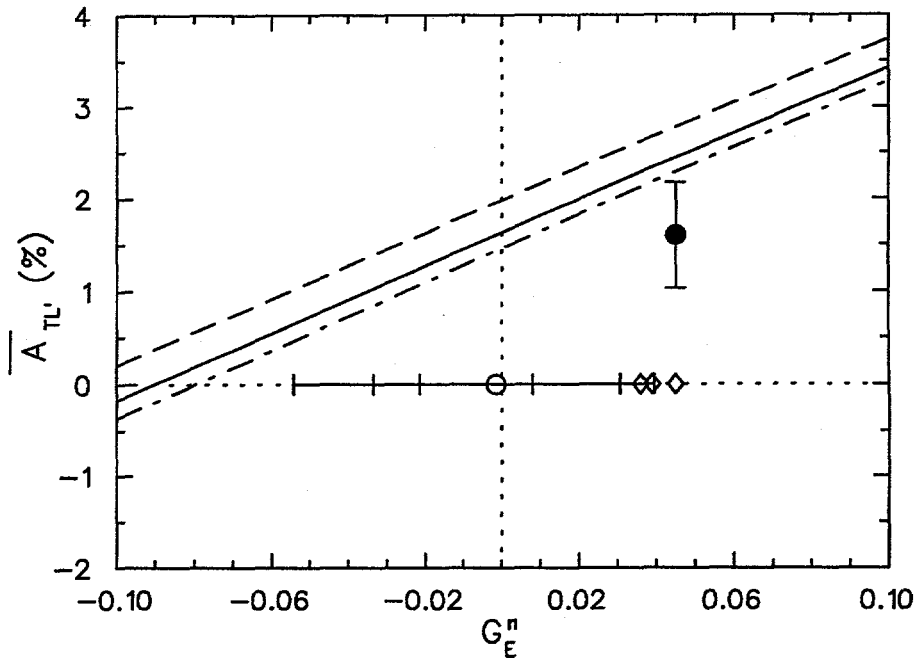

FIGURE 3. The predicted asymmetry $A_{TL'}$ in PWIA vs. G_E^n. The solid circle is the measured datum, and the open circle is the extracted G_E^n (see text).

In a completely analogous manner, the square of the neutron magnetic form factor, $G_M^{n\,2}$, can be extracted from the $A_{T'}$ data. In addition to the model dependences considered above, it was necessary to include the sensitivity of the $A_{T'}(G_M^{n\,2})$ predictions to different proton form factor parametrizations[27,26,28] in order to estimate the total theoretical uncertainty. In units of the dipole parametrization[27], $(\mu_n G_D)^2$, the result is[15]

$$\left(\frac{G_M^n}{\mu_n G_D}\right)^2 = 0.998 \pm 0.117 \pm 0.059 \pm 0.069 \qquad \text{at } Q^2 = 0.20\ (\text{GeV/c})^2, \quad (4)$$

where the errors are the experimental statistics, systematics, and combined theoretical NN potential, off-shell, and proton form factor uncertainties, respectively. The theoretical uncertainty given here is larger than that reported in Ref.[15] because additional contributions from NN potentials and off-shell prescriptions were considered here. The error from proton form factors alone is about ± 0.030.

The various predictions for $A_{TL'}(\omega)$ and $A_{T'}(\omega)$ are shown in Figs. 1 and 2. Calculation 1 with Galster form factors yields the solid curve. The upper dashed curve (maximum prediction) in Fig. 1 is obtained with calculation 2 and Gari-Krümpelmann form factors, while the lower dashed curve (minimum prediction) results from calculation 3 with Höhler form factors. Likewise, the upper dashed curve in Fig.

2 corresponds to calculation 2 with Höhler form factors, and the lower dashed curve is obtained with calculation 3 and Galster form factors.

5. Discussion

Two observations can be made: First, the results demonstrate that G_M^n can be successfully determined in inclusive scattering from $^3\vec{\mathrm{He}}$. The result (4) is in good agreement with theoretical predictions[27,26,28] as well as other experiments[5–7] done at similar Q^2. The error of the measurement is dominated by experimental statistics, and the residual systematic uncertainties are sufficiently small ($\lesssim \pm 10\%$) so that a precision measurement of G_M^n can be envisaged under improved experimental conditions in the near future. Even though the uncertainties of such a measurement are presently larger that those of the recent high-precision experiments with unpolarized deuterium[6–8], the $^3\vec{\mathrm{He}}$ technique is important in that it will provide valuable complementary information.

Second, an accurate determination of G_E^n in $^3\vec{\mathrm{He}}(\vec{e},e')$ appears to be rather difficult at the low Q^2 of the recent measurements. Although the experimental errors dominate, the residual theoretical uncertainty is substantial and in fact exceeds the differences between the various G_E^n predictions at this Q^2. At best, if experimental errors were absent, G_E^n could be determined with a precision similar to that of elastic electron-deuteron experiments[3], *i.e.* approximately $\pm 50\%$. An additional complication may arise from corrections to the PWIA: Recent, more sophisticated calculations, which include a full treatment of the trinucleon continuum[33,34], suggest that FSI corrections may be sizable for $A_{TL'}$ (but not for $A_{T'}$) in the low-Q^2 region.

Consequently, $^3\vec{\mathrm{He}}(\vec{e},e')$ is not a promising technique for the measurement of G_E^n at this Q^2. The success of the recent Mainz experiments[17,18] shows that precise data on G_E^n can be obtained in this kinematic region via the $^3\vec{\mathrm{He}}(\vec{e},e'n)$ reaction.

In going to higher Q^2, the PWIA model-dependent uncertainties in $^3\vec{\mathrm{He}}(\vec{e},e')$ are expected to become smaller, in particular because the proton contribution to $A_{TL'}$ decreases. In addition, the ability to distinguish different G_E^n parameterizations improves because the predictions diverge. To illustrate this point, we have extended the present PWIA analysis to $Q^2 = 1$ (GeV/c)^2. Keeping the electron scattering angle fixed at $\theta = 70°$ and varying the beam energy, asymmetry predictions were calculated as a function of G_E^n for different combinations of input parameters, as described above, and the residual theoretical uncertainty (due to NN potential and off-shell prescription) was estimated in the same manner as illustrated in Fig. 3. The result is shown as an error band in Fig. 4 along with several different parameterizations of G_E^n: Galster[27] (solid curve), the Platchkov fit[3] to $d(e,e')$ using the Paris potential (dashed curve), Gari-Krümpelmann[28] (long-dot-dashed curve), and Höhler[26] (short-dot-dashed curve). It should be emphasized that the error band shown is the estimated minimum *theoretical uncertainty only* and does not include experimental errors. One observes that $\pm 20\%$ precision may be achieved above $Q^2 \gtrsim 0.5$ (GeV/c)^2.

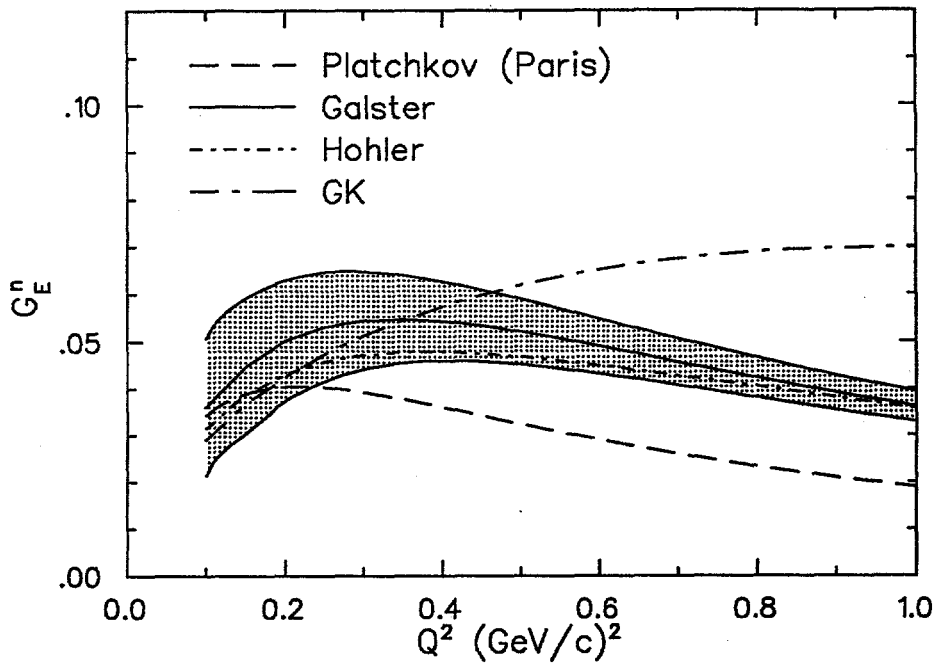

FIGURE 4. Estimated minimum theoretical uncertainty (shown as an error band) for the extraction of G_E^n from $^3\vec{\text{He}}(\vec{e}, e')$. The uncertainty, calculated in PWIA, is due to variations in NN potential and off-shell prescription. The curves represent various parameterizations of G_E^n.

The effect of FSI is expected to be negligible in this region[29].

6. Conclusions

In summary, the analysis of the spin-dependent asymmetries measured in a recent MIT-Bates $^3\vec{\text{He}}(\vec{e}, e')$ experiment at $Q^2 \simeq 0.2$ (GeV/c)^2 shows that $^3\vec{\text{He}}$ is a good effective polarized neutron target in the T' kinematics sensitive to G_M^n. The neutron magnetic form factor has been extracted from the data and is in agreement with the dipole parameterization. For the TL' kinematics sensitive to G_E^n, a detailed PWIA study shows a significant model uncertainty in which the sensitivity to G_E^n is masked by comparable sensitivities to NN potential model and off-shell prescription. Hence, $^3\vec{\text{He}}(\vec{e}, e')$ is not a promising technique for the measurement of G_E^n at this Q^2. However, the study also shows that relatively precise information on G_E^n ($\sim \pm 20\%$) can be extracted from inclusive experiments using $^3\vec{\text{He}}$ above a momentum transfer of $Q^2 \sim 0.5$ (GeV/c)^2.

7. Acknowledgements

I would like to thank Th. Bauer, F. Coester, T. W. Donnelly, C. Jones, R. Milner, R.-W. Schulze, and M. Titko for many useful comments and stimulating discussions. The efforts of M. Titko and R.-W. Schulze in providing the PWIA results, and of A. Stadler in calculating the $^3\vec{\text{He}}$ wave function for the various potential models, are gratefully acknowledged. This work was supported by the U.S. Department of Energy, Nuclear Physics Division, under contract No. W-31-109-ENG-38.

References

1. P. E. Bosted *et al.*, Phys. Rev. Lett. **68**, 3841 (1992).
2. A. Lung *et al.*, Phys. Rev. Lett. **70**, 718 (1993).
3. S. Platchkov *et al.*, Nucl. Phys. **A510**, 740 (1990).
4. S. Kopecky *et al.*, Phys. Rev. Lett. **74**, 2427 (1995).
5. P. Markovitz *et al.*, Phys. Rev. C **48**, R5 (1993).
6. H. Anklin *et al*, Phys. Lett. B **336**, 313 (1994).
7. E. E. W. Bruins *et al.*, Phys. Rev. Lett. **75**, 21 (1995).
8. Th. Bauer, these proceedings.
9. R. G. Arnold, C. E. Carlson, and F. Gross, Phys. Rev. C **23**, 363 (1981).
10. H. Arenhövel, Phys. Lett. B **199**, 13 (1987).
11. T. Eden *et al.*, Phys. Rev. C **50**, R1749 (1994).
12. F. Klein *et al.*, in *Proceedings of the VI Workshop on Perspectives in Nuclear Physics at Intermediate Energies*, ICTP, Trieste, May 1993 (World Scientific, Singapore, 1994).
13. C. E. Woodward *et al.*, Phys. Rev. Lett. **65**, 698 (1990); C. E. Jones *et al.*, Phys. Rev. C **47**, 110 (1993).
14. A. K. Thompson *et al.*, Phys. Rev. Lett. **68**, 2901 (1992).
15. H. Gao *et al.*, Phys. Rev. C **50**, R546 (1994).
16. J.-O. Hansen *et al.*, Phys. Rev. Lett. **74**, 654 (1995).
17. M. Meyerhoff *et al.*, Phys. Lett. B **327**, 201 (1994).
18. W. Heil, in *Proceedings of the IV International Symposium on Weak and Electromagnetic Interactions in Nuclei*, Osaka, Japan, 12-16 June 1995 (to be published).
19. T. W. Donnelly and A. S. Raskin, Ann. Phys. (N.Y.) **169**, 247 (1986).
20. B. Blankleider and R. M. Woloshyn, Phys. Rev. C **29**, 538 (1984).
21. C. Ciofi degli Atti, E. Pace, G. Salmè, Phys. Rev. C **51**, 1108 (1995).
22. R.-W. Schulze and P. U. Sauer, Phys. Rev. C **48**, 38 (1993).
23. R. G. Milner *et al.*, Nucl. Instr. Meth. **A274**, 56 (1989).
24. M. A. Titko, T. W. Donnelly, R.-W. Schulze, P. U. Sauer, A. Stadler, private communication (1994).

25. J. A. Caballero, T. W. Donnelly, and G. I. Poulis, Nucl. Phys. **A555**, 709 (1993).
26. G. Höhler *et al.*, Nucl. Phys. **B114**, 505 (1976).
27. S. Galster *et al.*, Nucl. Phys. **B32**, 221 (1971).
28. M. Gari and W. Krümpelmann, Phys. Lett. B **274**, 159 (1992); **282**, 483 (1992).
29. J. M. Laget, Phys. Lett. **B273**, 367 (1991); Phys. Lett. **B276**, 398 (1992).
30. M. Lacombe *et al.*, Phys. Rev. C **23**, 2405 (1981).
31. R. V. Reid, Ann. Phys. (N.Y.) **50**, 411 (1968).
32. R. Machleidt, Adv. Nucl. Phys. **19**, 189 (1989).
33. S. Ishikawa, in *Proceedings of the IV International Symposium on Weak and Electromagnetic Interactions in Nuclei*, Osaka, Japan, 12-16 June 1995 (to be published).
34. J. Carlson, private communication (1995).